Brain Advance Access published September 13, 2007

doi:10.1093/brain/awm205 *Brain* (2007) Page 1 of 14

Neurocognitive endophenotypes of obsessive-compulsive disorder

Lara Menzies,[1–3] Sophie Achard,[1] Samuel R. Chamberlain,[2–4] Naomi Fineberg,[2] Chi-Hua Chen,[1] Natalia del Campo,[3,4] Barbara J. Sahakian,[3,4] Trevor W. Robbins[3] and Ed Bullmore[1,3,5]

[1]Brain Mapping Unit, University of Cambridge, [2]Department of Psychiatry, Queen Elizabeth II Hospital, Welwyn Garden City, [3]Department of Experimental Psychology, Behavioural and Clinical Neurosciences Institute, University of Cambridge, Cambridge, CB2 3EB, [4]Department of Psychiatry, Addenbrooke's Hospital, Cambridge, CB2 2QQ and [5]Clinical Unit Cambridge, Addenbrooke's Centre for Clinical Investigations, Clinical Pharmacology & Discovery Medicine, GlaxoSmithKline, Cambridge CB2 2QQ, UK

Correspondence to: Professor Ed Bullmore, Brain Mapping Unit, Department of Psychiatry, University of Cambridge, Addenbrooke's Hospital, Cambridge, CB2 2QQ, UK
E-mail: etb23@cam.ac.uk

Endophenotypes (intermediate phenotypes) are objective, heritable, quantitative traits hypothesized to represent genetic risk for polygenic disorders at more biologically tractable levels than distal behavioural and clinical phenotypes. It is theorized that endophenotype models of disease will help to clarify both diagnostic classification and aetiological understanding of complex brain disorders such as obsessive-compulsive disorder (OCD). To investigate endophenotypes in OCD, we measured brain structure using magnetic resonance imaging (MRI), and behavioural performance on a response inhibition task (Stop-Signal) in 31 OCD patients, 31 of their unaffected first-degree relatives, and 31 unrelated matched controls. Both patients and relatives had delayed response inhibition on the Stop-Signal task compared with healthy controls. We used a multivoxel analysis method (partial least squares) to identify large-scale brain systems in which anatomical variation was associated with variation in performance on the response inhibition task. Behavioural impairment on the Stop-Signal task, occurring predominantly in patients and relatives, was significantly associated with reduced grey matter in orbitofrontal and right inferior frontal regions and increased grey matter in cingulate, parietal and striatal regions. A novel permutation test indicated significant familial effects on variation of the MRI markers of inhibitory processing, supporting the candidacy of these brain structural systems as endophenotypes of OCD. In summary, structural variation in large-scale brain systems related to motor inhibitory control may mediate genetic risk for OCD, representing the first evidence for a neurocognitive endophenotype of OCD.

Keywords: neuroimaging; inhibition; obsessive-compulsive; multivoxel; familial

Abbreviations: ANOVA = analysis of variance; DLPFC = dorsolateral prefrontal cortex; LSD = Least Significant Difference; MADRS = Montgomery Asberg Depression Rating Scale; MNI = Montreal Neurological Institute; MRI = magnetic resonance imaging; NART = National Adult Reading Test; OCD = obsessive-compulsive disorder; OCI-R = Obsessive Compulsive Inventory - Revised; OFC = orbitofrontal cortex; PLS = partial least squares; QTL = quantitative trait locus; RIFG = right inferior frontal gyrus; SPECT = Single Photon Emission Computed Tomography; SSRT = stop-signal reaction time; YBOCS = Yale Brown Obsessive Compulsive Scale

Received April 16, 2007. Revised July 30, 2007. Accepted July 31, 2007

Introduction

An endophenotype was originally defined in the 1960s as a 'measurable component unseen by the unaided eye on the pathway between disease (phenotype) and distal genotype' (John and Lewis, 1966; Gottesman and Shields, 1973). It is a heritable quantitative trait associated with increased genetic risk for a disorder and therefore present in both patients and their clinically unaffected relatives (Gottesman and Gould, 2003; Bearden and Freimer, 2006). Interest in endophenotypes (or intermediate phenotypes) has been stimulated by the difficulties encountered in establishing specific genetic causes for complex disorders by classical linkage or association designs. Although most major psychiatric syndromes are highly heritable, several decades of effort to discover causative genes has yielded disappointing results. It is argued that traditional clinical phenotypes, such as a

diagnosis of schizophrenia or obsessive-compulsive disorder (OCD), likely subtend considerable genetic heterogeneity in pathogenetic mechanisms and are too far 'downstream' from sites of gene action to support statistically powerful and replicable linkage to chromosomal loci or association with specific allelic variation (Leboyer *et al.*, 1998; Bearden *et al.*, 2004). In this context, endophenotypes offer an attractive strategy for discovering susceptibility genes since they represent deconstruction of the clinical phenotype into biological variables hypothetically more proximal to genetic effects.

Neuroimaging measurements have obvious potential interest as endophenotypes for neuropsychiatric disorders. Healthy twin studies have shown that brain structure is highly heritable (Thompson *et al.*, 2001; Wright *et al.*, 2002) and brain structural abnormalities have been described in case-control studies of most major psychiatric syndromes. Several experimental designs have been adopted to identify structural magnetic resonance imaging (MRI) endophenotypes of psychiatric syndromes. A common approach has been to identify MRI markers that are abnormal in clinically unaffected relatives of patients with the index disorder, compared to unrelated healthy volunteers. More complex designs have included studies of probands and relatives drawn from multiplex families, where each individual could be assigned an estimate of genetic risk for a disorder and MRI endophenotypes were then defined as grey or white matter systems covarying significantly with this risk (McDonald *et al.*, 2004). Sib-pair designs, where endophenotypes are identified by reduced variability within genetically related pairs (one proband and one unaffected relative), have not yet been widely used in MRI studies of neuropsychiatric syndromes, but see Marcelis *et al.* (2003).

Obsessive-compulsive disorder (OCD) is a heritable neuropsychiatric disorder with a lifetime prevalence of 2–3% (Karno *et al.*, 1988; Weissman *et al.*, 1994). Evidence for a genetic contribution to aetiology is provided by twin studies (Inouye, 1965; Carey and Gottesman, 1981), and family studies showing that the disorder is 5–7 times more frequent in first-degree relatives of patients than controls (Pauls *et al.*, 1995; Nestadt *et al.*, 2000). OCD is a major cause of social and occupational disability with considerable associated economic costs; ~$8.4 billion/year in the US (DuPont *et al.*, 1995). It is clinically characterized by two symptom dimensions: *obsessions*, which are unwanted, intrusive, recurrent thoughts often concerned with contamination, checking or symmetry; and *compulsions*, which are repetitive behaviours carried out in relation to obsessions e.g. washing, household safety checking and object rearrangement (DSM-IV; American Psychiatric Association, 1994). It is increasingly clear that such classic obsessive-compulsive symptoms are associated with a pattern of cognitive impairments, suggesting that the perseverative thoughts and behaviours that are symptomatic of the disorder may reflect a loss of normal inhibitory processes (Chamberlain *et al.*, 2005).

According to theoretical models of OCD, symptoms and associated cognitive impairments emerge from disordered structure and function of large-scale neurocognitive networks, specifically 'limbic' or 'affective' cortico-striato-thalamic circuits including orbitofrontal cortex (OFC) (Graybiel and Rauch, 2000; Saxena *et al.*, 2001). These circuits, first identified by anatomical studies in primates (Alexander *et al.*, 1986; Lawrence *et al.*, 1998), have been implicated in the pathophysiology of OCD by human imaging and lesion-based studies (Rapoport and Wise, 1988; Saxena, 2003). The most consistent finding from structural MRI measurements of selected regions-of-interest has been reduced grey matter volume of OFC in patients with OCD; there is less consistent evidence in support of volume changes in caudate nucleus, medial temporal lobe structures, and anterior cingulate cortex (Scarone *et al.*, 1992; Robinson *et al.*, 1995; Aylward *et al.*, 1996; Jenike *et al.*, 1996; Rosenberg and Keshavan, 1998; Szeszko *et al.*, 1999; Gilbert *et al.*, 2000; Kwon *et al.*, 2003; Choi *et al.*, 2004, 2006; Kang *et al.*, 2004; Szeszko *et al.*, 2004; Atmaca *et al.*, 2007); see Supplementary Fig. 1 for detail.

More recently, studies have used computational techniques, such as voxel-based morphometry (Ashburner and Friston, 2000), to map local structural differences in case-control designs without restriction *a priori* to selected regions (Kim *et al.*, 2001; Pujol *et al.*, 2004; Valente *et al.*, 2005). However, the few studies adopting this approach to date have produced inconsistent results (see Supplementary Fig. 2). There are various possible reasons for the limited replicability of imaging studies of OCD, including clinical heterogeneity or co-morbidity of patient samples, medication effects and small sample sizes in the context of conservative significance thresholds mandated by the large number of voxels to be tested in a whole brain approach. Another possibility is that regional or voxel level analysis, focused on local changes in brain structure, may be less than optimally powerful to detect case-control differences in brain structure which are theoretically expected at the more distributed level of large-scale neurocognitive systems.

Two prior imaging studies have used theoretically more appropriate methods designed to characterize brain abnormalities associated with OCD at a systems level. Soriano-Mas *et al.* (2007) described a whole brain profile of anatomical abnormality in patients with OCD compared to healthy controls by testing the sum of *t*-statistics over all voxels against a chi-square distribution (Worsley *et al.*, 1995, 1997). Harrison *et al.* (2006) used a non-parametric test in conjunction with canonical variates analysis [implemented using NPAIRS software (Strother *et al.*, 2002)] to identify a cortico-striatal system of abnormal brain activation in patients with OCD performing the Stroop task during PET scanning. This study also demonstrated relatively greater power of this multivariate method

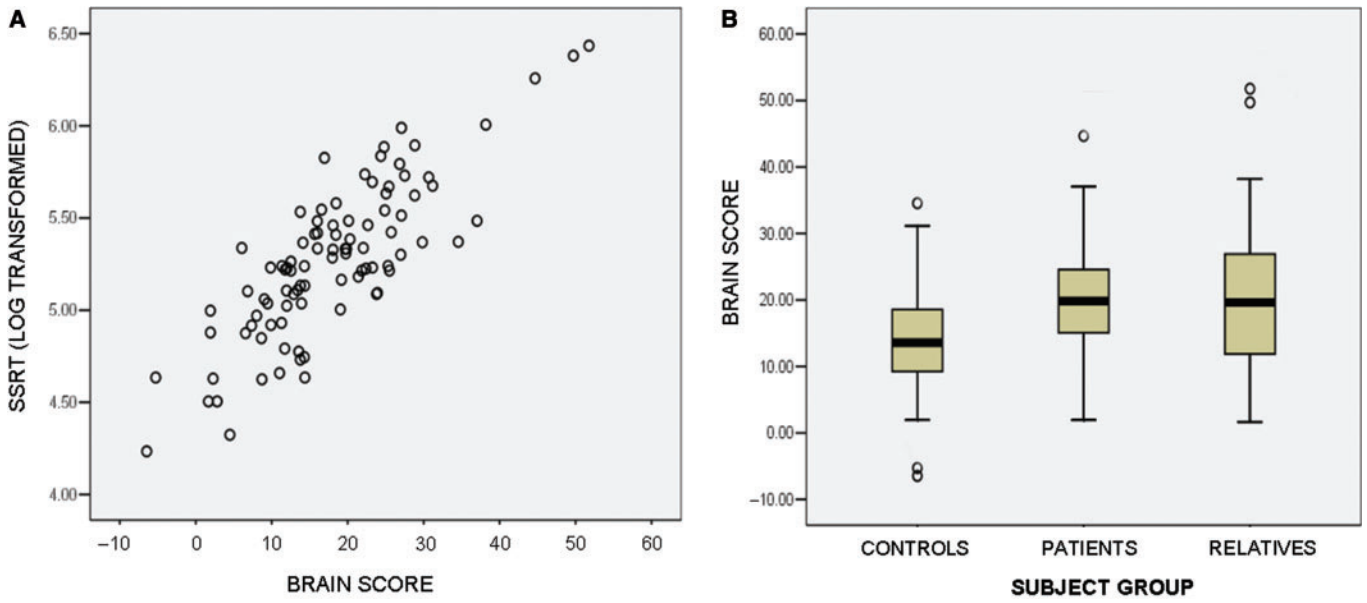

Fig. 1 Motor inhibitory behaviour (stop-signal reaction time; SSRT) and associated brain scores (summary measures of grey matter correlation with SSRT over the whole brain). (**A**) Scatter plot showing the relationship between brain score (*x*-axis) and log-transformed SSRT (*y*-axis); Pearson's $r = 0.82$, $N = 93$, $P < 0.001$. (**B**) Boxplots of brain score by group showing significantly larger scores for both patients and relatives compared to controls. For each boxplot, thick bar indicates median; box and whiskers represent interquartile range and range, respectively.

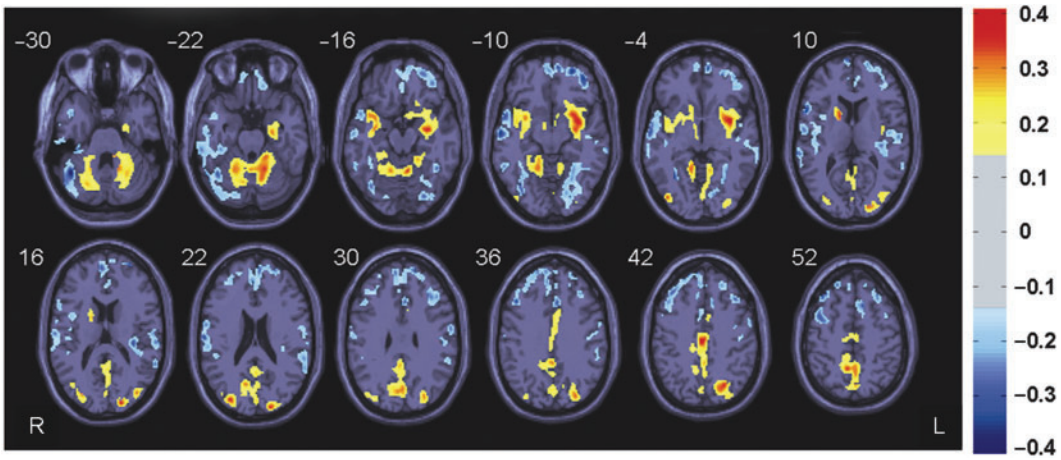

Fig. 2 Brain maps illustrating regions where grey matter density was most strongly correlated with latency of motor inhibitory response (SSRT). Red/yellow regions indicate areas in which increased grey matter density is associated with prolonged SSRT (impaired response inhibition); blue regions indicate areas where decreased grey matter density is associated with prolonged SSRT. Colour bar indicates strength of correlation between SSRT and grey matter density for each voxel; R and L markers indicate side of the brain, numbers denote the *z* dimension of each slice in MNI space.

to detect brain functional abnormalities when compared to the results of a more traditional mass or multiple univariate approach to analysis, entailing a significance test at each individual voxel (Harrison *et al.*, 2006). However, no prior MRI studies have provided evidence for heritability or familiality of brain structural abnormalities in OCD, as is required to support the candidacy of neurocognitive systems as endophenotypes of OCD.

In this context, we were motivated to address four key hypotheses: (i) that motor response inhibition is abnormal in patients with OCD and their first-degree relatives; (ii) that variation in motor inhibition is associated with structural variation in large-scale brain systems identified by a multivoxel analysis of MRI data; (iii) that patients with OCD and their first-degree relatives have abnormal grey matter density in these motor inhibition systems, likely including orbitofronto-striatal regions previously implicated in OCD and (iv) that there are familial effects on variation in inhibitory function and associated brain systems.

To test these predictions, we estimated the stop-signal reaction time (SSRT) using a well-validated stop-signal task (Logan *et al*., 1984), and acquired structural MRI data, in patients with OCD, their unaffected first-degree relatives, and healthy volunteers. The available evidence suggests structural abnormalities at a systems level in OCD, and prior functional imaging studies of motor inhibition indicate this processes is subserved by an 'inhibitory neurocognitive network' (Rubia *et al*., 2001b). Therefore, we used the statistical method of partial least squares (PLS) (McIntosh *et al*., 1996; McIntosh and Lobaugh, 2004), in an innovative application to structural neuroimaging data, to identify grey matter systems (comprising multiple voxels) maximally correlated with variation in SSRT. Finally, we assessed the familiality of cognitive and MRI markers by a permutation test of their variation within proband–relative pairs, each pair comprising a patient with OCD and their clinically unaffected first-degree relative.

Materials and Methods

Participants and clinical assessments

The sample comprised 31 patients with a diagnosis of OCD, 31 unaffected first-degree relatives of a patient with OCD, and 31 unrelated healthy volunteers (including 30 complete pairs of a proband and their first-degree relative). Patients were recruited from an outpatient service by a consultant psychiatrist (NF) and satisfied DSM-IV criteria (American Psychiatric Association, 1994) for a diagnosis of OCD. Patients with symptoms of excessive washing or checking, in the absence of hoarding or motor tics, were selected by clinical interview, using a well-validated screening instrument; the YBOCS Symptom Checklist (Goodman *et al*., 1989). This careful clinical screening process was adopted to minimize co-morbidity and maximize symptomatic homogeneity in the patient sample selected for subsequent assessment by cognitive testing and MRI, since there is evidence that OCD subgroups with different symptom profiles may have different underlying profiles of brain abnormality (Mataix-Cols *et al*., 2004).

Eligible patients gave consent for a first-degree relative to be contacted (preferably a similarly aged sibling; alternatively a parent or child). Unrelated healthy volunteers were recruited by local community advertisements.

Participants were excluded if they had an axis I psychiatric disorder (apart from OCD in the patients), serious head injury, substance abuse, epilepsy or MRI contraindications.

The Mini International Neuropsychiatric Inventory (MINI) (Sheehan *et al*., 1998) was used to screen for axis I psychiatric disorders; the Montgomery–Asberg depression rating scale (MADRS) (Montgomery and Asberg, 1979) to measure current depressive symptoms; and two instruments, the clinician-rated yale-brown obsessive compulsive scale (YBOCS) (Goodman *et al*., 1989) and the self-rated obsessive compulsive inventory-revised (OCI-R) (Foa *et al*., 2002), were used to measure obsessive-compulsive symptom severity. Verbal IQ was estimated using the National Adult Reading Test (NART) (Nelson, 1982).

Patients were clinically medicated as follows: 21 were prescribed selective serotonin reuptake inhibitors; 1 was prescribed clomipramine and 1 was prescribed quetiapine. Eight patients were unmedicated. Relatives and healthy volunteers were not taking psychotropic medication.

All participants gave written informed consent and the study was approved by the Addenbrooke's NHS Trust Local Research Ethics Committee (Cambridge, UK). Behavioural performance on this motor inhibition task was previously reported for a subset of the individuals in this sample (Chamberlain *et al*., 2007). Here we report for the first time both behavioural and MRI data on the full sample.

Behavioural testing

We used a computerized version of the stop-signal task to assess inhibition of prepotent motor responses (Logan *et al*., 1984); for a full description see Aron *et al*. (2003*a*). Briefly, participants watched a computer screen on which a series of five blocks of 64 arrows per block were visually presented. Arrows pointed either to the right (50%) or the left (50%) and subjects responded accordingly by pressing the appropriate button; the order of presentation of right- and left-pointing arrows was randomized. In a randomly assigned proportion (25%) of trials, an audible stop-signal was heard after presentation of the arrow and subjects were instructed to inhibit their motor response to these trials. The interstimulus interval (ISI) and the stop-signal delay were varied according to the subject's performance such that subjects were able successfully to inhibit their responses to 50% of the stop trials. From these behavioural data, the stop-signal reaction time (SSRT, ms), i.e. the processing time required to inhibit a prepotent motor response, was calculated for each subject. SSRT data were normalized by log transformation before statistical analysis in SPSS v11 for Windows.

MRI data acquisition

Structural MRI data were obtained using a GE Signa system (General Electric, Milwaukee, USA) operating at 1.5T in the Magnetic Resonance Imaging and Spectroscopy Unit, Addenbrooke's Hospital, Cambridge, UK. Axial 3D T1-weighted images were acquired using a spoiled gradient recall (SPGR) sequence and the following parameters: number of slices = 124, slice thickness = 2 mm, TR = 33 ms, TE = 3 ms, field of view = 24 cm, flip angle = 40°, matrix size 256 × 256, voxel dimensions = 0.94 mm × 0.94 mm; scanning time = 20 min. In addition, axial dual-echo, fast spin echo (T2- and PD-weighted) images were acquired with number of slices = 40, slice thickness = 4 mm, TR = 5625 ms, TE = 20 and 102 ms with an 8-echo train length, field of view = 24 cm, matrix size = 256 × 256, voxel dimensions = 0.94 mm × 0.94 mm; scanning time = 10 min. Total scanning time (including a localizer scan and a diffusion tensor imaging sequence not reported here) amounted to 40 min.

MRI data analysis: pre-processing

First, non-brain tissue was removed using an automated brain extraction procedure (Smith, 2002). The T1-, T2- and PD-weighted images were then segmented using a multichannel tissue classification algorithm and probabilistic maps of grey matter, white matter, CSF and dural tissues were created by estimating the partial volume coefficient for each voxel, which represents the probability of each voxel belonging to one of four tissue classes (Zhang *et al*., 2001). The segmented grey matter partial-volume maps were registered in Montreal Neurological

Institute (MNI) standard space by an affine transformation using a segmented grey matter template in FSL (Sheehan *et al.*, 1998; Jenkinson and Smith, 2001; Jenkinson *et al.*, 2002). The registered data were spatially smoothed by a 2D Gaussian kernel with full width at half maximum (FWHM) = 3 mm. All preprocessing was performed using FSL software (http://www.fmrib.ox.ac.uk/fsl).

MRI data analysis: partial least squares

To identify grey matter systems optimally correlated with SSRT, we used the statistical technique of partial least squares; PLS (McIntosh *et al.*, 1996). For implementation, we used PLSGUI software (http://www.rotman-baycrest.on.ca/pls/) running in MatLab.

Briefly, over all participants, we estimated the correlations between log-transformed SSRT scores and normalized grey matter density at each voxel in the registered images where the probability of grey matter $P(\mathrm{GM})$ was greater than 0.1 (thus excluding from consideration all voxels representing predominantly white matter or CSF). The normalization of grey matter density involved dividing each voxel's density estimate by the mean density of grey matter over all voxels in the brain (thus correcting individual voxel values for between-subject differences in global grey matter volume). The overall strength of correlation between grey matter density and SSRT was summarized by the scalar $d = \sqrt{\sum (r_i)^2}$, where r_i is the correlation at the ith voxel and the sum is over all $i = 1,2,3,\ldots V$ voxels with $P(\mathrm{GM}) > 0.1$. The brain score for each participant was calculated as the sum of grey matter probabilities multiplied by the local weighted correlations with SSRT: i.e. $B(j) = \sum P(\mathrm{GM})_{i,j} * r_i / d$, where $B(j)$ is the brain score for the jth participant, $P(\mathrm{GM})_{i,j}$ is the probability of grey matter at the ith voxel for the jth participant, and the sum is over all V voxels for each participant.

The association between grey matter probability and SSRT was tested for statistical significance by a permutation test of d. The ordering of SSRT scores was randomly permuted before recalculation of the correlations with grey matter at each voxel, leading to an estimate of d under the null hypothesis. This process was repeated 1000 times to sample the permutation distribution of d and the observed value was compared to the 950th value of the ranked permutation distribution for a test with one-tailed probability of type 1 error, $P = 0.05$. Brain scores were also compared between groups by analysis of variance (ANOVA) and *post hoc* testing (SPSS v11 for Windows).

The anatomical configuration of brain systems strongly associated with SSRT was visualized by thresholding the correlations at each voxel with an arbitrary threshold, $|r_i| > 0.14$ and a minimum cluster size of 400 voxels. This cluster size threshold was chosen for illustrative purposes, to best demonstrate the large-scale anatomical covariation with SSRT scores. The choice of visualization thresholds makes no difference to the statistical significance of d (the overall strength of correlation between grey matter density and SSRT) or the calculation of brain scores for each participant.

We also used this thresholded set of correlated voxels as a 'mask', applied to the preprocessed maps of grey matter probability, to estimate the grey matter density represented by the thresholded system and its component regions in each participant. These measures of regional grey matter density were also compared between groups by ANOVA and *post hoc* testing.

Assessment of familiality

We used two complementary techniques to assess the familiality of SSRT scores, or related grey matter systems (brain score and grey matter density), in the OCD patients and their first-degree relatives. First, we calculated the variance of the within-pair difference in SSRT (or brain scores or grey matter density): $\sigma[\mathrm{proband} - \mathrm{relative\ pair}] = \sum (u_i - \bar{u})^2 / N$ where u_j is the observed within-pair difference of the measure for the jth pair of participants, $\bar{u}$ is the mean within-pair difference and N is the total number of pairs ($N = 30$). Then we randomly reassigned the observations to new pairs, so that each patient was now paired with a clinically unaffected individual to whom they were not personally related. We recalculated the variance of the within-pair difference in phenotype after each random permutation and repeated this process 100 000 times to sample the permutation distribution of σ[proband–relative pair] under the null hypothesis that the observed variance in within-pair differences was not determined by the familial relatedness of the observed pairs. On the alternative hypothesis that the observed variance would be small, we compared it to the 5000th value of the permutation distribution for a test with one-tailed $P < 0.05$.

Second, as another exploration of the similarity between patients and their relatives on behavioural and brain-based measures, we examined the strength and significance of the within-pair correlation of SSRT, brain score and grey matter densities between patients and their own relatives. We used within-pair correlation rather than intraclass correlation because there was a natural ordering (patient or relative) within each pair.

Results

Demographic and clinical data

The three groups were well matched for age, verbal IQ, gender and handedness (Table 1). As expected, there were significant differences between groups on both measures of obsessive-compulsive symptom severity (YBOCS: ANOVA, $F_{2,90} = 337$, $P < 0.001$; OCIR: ANOVA, $F_{2,86} = 58.0$, $P < 0.001$). *Post hoc* least significant difference (LSD) tests confirmed that patients scored significantly higher on both instruments than either healthy volunteers (YBOCS: df = 60, $P < 0.001$; OCIR: df = 57, $P < 0.001$) or relatives (YBOCS: df = 60, $P < 0.001$; OCIR: df = 56, $P < 0.001$); whereas relatives did not differ significantly from healthy volunteers on either instrument (YBOCS: df = 60, $P = 0.08$; OCIR: df = 59, $P = 0.54$). Although mean depressive symptom severity scores measured using MADRS were below the threshold for a diagnosis of depressive disorder in all three groups, patients with OCD had higher scores than relatives and healthy volunteers (ANOVA, $F_{2,90} = 14.2$, $P < 0.001$; LSD tests, patients compared with healthy volunteers: df = 60, $P < 0.001$; patients compared with relatives: df = 60, $P < 0.001$). Relatives did not differ from healthy volunteers (df = 60, $P = 0.36$) (Table 1).

Stop-signal task performance

There was a significant difference between groups in mean SSRT (ANOVA, $F_{2,90} = 9.07$, $P < 0.001$) (Table 1). *Post hoc* analysis demonstrated that both patients (df = 60, $P = 0.001$)

Table 1 Demographic, clinical and behavioural data for patients with OCD, their first-degree relatives and healthy, unrelated volunteers

Variable	OCD patients ($N = 31$)		First-degree relatives ($N = 31$)		Healthy unrelated volunteers ($N = 31$)		Analysis	
	Mean	SD	Mean	SD	Mean	SD	F (df = 2,90)[a]	*P*
Demographic data								
Age (years)	32.5	11.1	36.7	13.4	33.4	11.1	1.03	0.36
Handedness (right:left)	27:3		26:4		24:7			0.44[b]
Gender (male:female)	9:22		9:22		11:20			0.82[c]
NART	113.3	7.0	114.4	8.7	115.9	6.4	0.91	0.41
Clinical data								
YBOCS	21.9	5.5	1.7	3.3	0	0	336.5	<0.001
OCI-R	36.5	18.3	7.1	10.8	5.16	4.9	58.0	<0.001
MADRS	5.6	6.3	1.5	2.6	0.5	1.1	14.2	<0.001
Age of onset of symptoms (years)	15.6	8.7						
Duration of illness (years)	16.4	11.7						
Cognitive data								
SSRT (log transformed)	5.36	0.34	5.42	0.43	5.03	0.38	9.07	<0.001
Median 'go' reaction time (ms)	457	103	406	124	403	68.4	2.76	0.07

Abbreviations; OCD; obsessive-compulsive disorder, SD; standard deviation.
[a]df = 2, 89 for NART and df = 2, 86 for OCI-R due to data unavailability.
[b]Fisher's exact test, total $N = 91$ due to data unavailability.
[c]χ^2 test, df = 2.

and relatives (df = 60, $P < 0.001$) had significantly greater SSRT than healthy volunteers. There was no significant difference in SSRT between patients and relatives (df = 60, $P = 0.50$). Of note, these between-group differences in response inhibition were not accompanied by significant non-specific latency differences in responding to uninhibited trials (median 'go' reaction time: ANOVA, $F_{2,90} = 2.76$, $P = 0.07$). Additionally, there was no significant correlation between age and SSRT in relatives ($r = 0.18$, $N = 31$, $P = 0.33$), excluding the possibility that younger relatives perform worse on the task and might therefore represent individuals with an OCD prodrome.

Grey matter systems correlated with SSRT

There was a significant correlation between SSRT and grey matter probability ($d = 44.9$, permutation test, $P = 0.05$) and individual brain scores were strongly positively correlated with SSRT ($r = 0.82$, $N = 93$, $P < 0.001$) (Fig. 1A). As expected, brain scores were significantly different between groups (ANOVA, $F_{2,90} = 4.18$, $P = 0.018$) (Fig. 1B) and *post hoc* analysis demonstrated that this was due to significantly greater brain scores in patients compared to healthy volunteers (df = 60, $P = 0.021$) and in relatives compared to healthy volunteers (df = 60, $P = 0.010$); there was no significant difference in brain scores between patients and relatives (df = 60, $P = 0.78$).

An anatomical map of voxels strongly correlated with SSRT over all participants highlighted two extensive systems which were, respectively, positively and negatively correlated with latency of inhibitory processing (Fig. 2). In the positively correlated system, longer SSRT was associated with *increased* grey matter probability. This predominantly parieto-cingulo-striatal system comprised middle and posterior cingulate cortices (approximate Brodmann areas [BA] 23, 24, 31), bilateral putamen/caudate and amygdala, bilateral parietal cortical areas (BA 39, 40) and bilateral cerebellum. In the negatively correlated system, longer SSRT was associated with *decreased* grey matter probability. This predominantly frontal system comprised bilateral middle and medial orbitofrontal cortex (BA 11, 47), inferior frontal gyri (BA 44, 45), superior frontal and premotor cortices (BA 6, 8, 9), anterior cingulate cortex (BA 32) and bilateral temporal cortical areas (BA 21, 22, 37, 42) (Table 2).

To explore these results further, we extracted grey matter values for the systems in Fig. 2 that were correlated with SSRT. We confirmed that grey matter density in the parieto-cingulo-striatal system was positively correlated with SSRT ($r = 0.70$, $N = 93$, $P < 0.001$), grey matter density in the frontal system was negatively correlated with SSRT ($r = -0.78$, $N = 93$, $P < 0.001$), and grey matter density in the two systems was negatively correlated with each other ($r = -0.78$, $N = 93$, $P < 0.001$), indicating that individuals with prolonged SSRT and larger positive brain scores (typically patients and relatives) tended to have *both* increased grey matter in the parieto-cingulo-striatal system *and* reduced grey matter in the frontal system.

There were significant between-group differences in grey matter probability measured in both the parieto-cingulo-striatal system (ANOVA, $F_{2,90} = 4.27$, $P = 0.017$) and frontal system (ANOVA, $F_{2,90} = 3.36$, $P = 0.039$). When we explored

Table 2 Anatomical details for brain regions where grey matter density was positively or negatively correlated with stop–signal reaction time (SSRT)

Cluster number	Size (voxels)	Peak correlation (*r*)	MNI coordinates (mm)			Region
			X	*Y*	*Z*	
Red regions (positive correlation between grey matter density per voxel and SSRT)						
1	4172	0.408	0	−20	40	Mid cingulate gyrus (BA 23, 24)
			0	−50	30	Posterior cingulate gyrus (BA 24, 31)
			−2	−56	22	Precuneus (BA 7)
			8	−58	2	R Lingual gyrus (BA 18)
			−8	−72	2	L Lingual gyrus (BA 30)
2	1720	0.373	−26	6	−8	L putamen
			−12	8	−12	L caudate
			−28	−6	−14	L amygdala
			−30	−12	−20	L hippocampus
3	1016	0.360	−22	−92	20	L superior occipital gyrus (BA 19)
			−30	−70	44	L inferior lateral parietal lobe (BA 40, 7)
4	1176	0.344	12	8	10	R caudate
			18	2	−6	R globus pallidus
			30	2	−8	R putamen
			26	−4	−14	R amygdala
			44	−4	−12	R superior temporal gyrus (BA 38)
5	486	0.341	28	−84	22	R mid occipital gyrus (BA 18, 19)
			42	−78	32	R angular gyrus (BA 39)
6	3882	0.340	−34	−56	−34	L cerebellar hemisphere
			24	−82	−48	R cerebellar hemisphere
			−4	−76	−40	Cerebellar vermis
			12	−52	−6	R lingual gyrus (BA 19)
			−14	−60	−6	L lingual gyrus (BA 19)
Blue regions (negative correlation between grey matter density per voxel and SSRT)						
7	1398	−0.407	40	−60	−30	R cerebellar hemisphere
8	1665	−0.371	58	−4	22	R postcentral gyrus (BA 40, 43)
			56	0	20	R precentral gyrus (BA 4, 6)
			60	−18	20	R supramarginal gyrus (BA 40)
9	2410	−0.357	−26	54	−12	L mid/medial orbitofrontal cortex (BA 11, 47)
			10	38	−20	R mid/medial orbitofrontal cortex (BA 11, 47)
			−52	34	−2	L inferior frontal gyrus pars triangularis (BA 44, 45)
10	1331	−0.354	52	14	10	R inferior frontal gyrus pars opercularis (BA 44, 45)
			58	−14	−10	R mid temporal gyrus (BA 20, 21)
			46	−10	6	R insula
11	1188	−0.328	−12	14	48	L superior frontal gyrus (BA 8, 6)
			−2	8	48	Bilateral supplementary motor area (BA 8, 6)
			−6	22	30	Medial frontal gyrus/anterior cingulate (BA 32)
12	1900	−0.311	40	22	38	R mid frontal gyrus (BA 6, 8, 9)
13	1715	−0.309	−52	−26	6	L superior temporal gyrus (BA 22, 42)
			−38	−22	14	L insula
14	873	−0.292	−46	−52	−14	L inferior temporal gyrus (BA 21, 37)

Abbreviations: BA = Brodmann's area; L = left; R = right.

group differences separately for each anatomically distinct region in each system, we found that left inferior parietal and dorsal occipital regions demonstrated the greatest between-group difference in grey matter probability among all regions comprising the system positively correlated with SRRT (ANOVA, $F_{2,90} = 7.48$, $P = 0.001$); whereas bilateral orbitofrontal cortex demonstrated the greatest between-group difference among all regions comprising the system negatively correlated with SSRT (ANOVA, $F_{2,90} = 4.92$, $P = 0.009$) (Table 2, Fig. 3). There were no regions in which there were significant differences in grey matter between patients and relatives (LSD; df = 60, $P > 0.1$).

Familiality of cognitive and neuroimaging phenotypes

By a permutation test of the variance of within-pair differences in brain scores, we were able to show that the observed within-pair variance was small (σ[proband–relative pair] = 127) compared to the distribution of variances in a

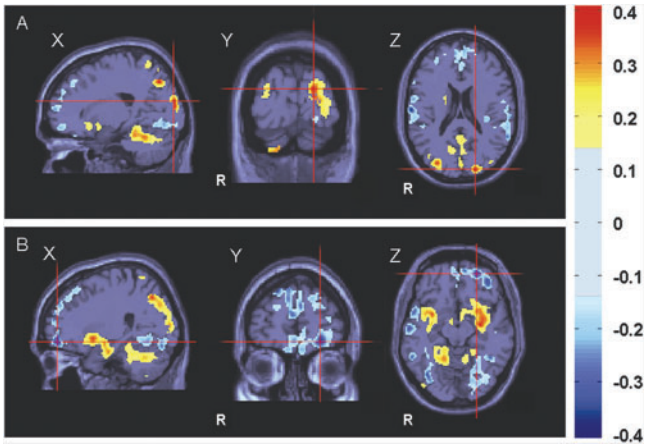

Fig. 3 Brain maps highlighting regions of most significant group difference in grey matter density between OCD patients and first-degree relatives compared to healthy volunteers. (**A**) Most significant red regions were in left occipital and inferior parietal areas (BA 19, 40) (Table 2; cluster 3); one way ANOVA ($F_{2,90} = 7.48$, $P = 0.001$), *post hoc* tests; patients versus healthy volunteers; $P = 0.002$, relatives versus healthy volunteers; $P = 0.001$, patients versus relatives; $P = 0.85$. (**B**) Most significant blue regions were in bilateral orbitofrontal and left inferior frontal gyral regions (Table 2; cluster 9) (BA 11, 44, 45, 47); one way ANOVA ($F_{2,90} = 4.92$, $P = 0.009$), *post hoc* tests; patients versus healthy volunteers; $P = 0.013$, relatives versus healthy volunteers; $P = 0.005$, patients versus relatives; $P = 0.76$. R marker indicates right side of the brain; *x*, *y*, and *z* indicate planes of brain maps; cross-hairs indicate point of peak correlation with the behavioural measure (SSRT).

sample of 100 000 randomly permuted pairs of patients and first-degree relatives (permutation test, $P = 0.014$) (Fig. 4A). This observation is compatible with the (alternative) hypothesis that variance of true proband–relative pair differences is smaller because the phenotype in question, e.g. brain scores, is determined by familial factors in common to both the patient and the first-degree relative in each pair.

We applied the same permutation test to analyses of the variance of within-pair differences in grey matter density of the parieto-cingulo-striatal system positively correlated with SSRT and in grey matter density of the frontal system negatively correlated with SSRT. In both cases, we found that the observed within-pair variance was significantly small compared to the appropriate permutation distributions (permutation tests, $P = 0.009$ and $P = 0.015$, respectively), again implying that familial factors shared between patients and relatives determined grey matter volume in these systems. Interestingly, applying the same approach to analysis of the SSRT scores, provided no evidence for significantly reduced variance of within-pair differences on this cognitive measure (permutation test, $P = 0.25$).

A broadly consistent pattern of results was obtained by analysis of correlation between patients and their relatives: these were significantly different from zero for brain score ($r = 0.41$, $N = 30$, $P = 0.023$), mean grey matter probability in the parieto-cingulo-striatal system ($r = 0.46$, $N = 30$, $P = 0.012$) and mean grey matter probability in the frontal system ($r = 0.42$, $N = 30$, $P = 0.022$). In contrast, there was no significant within-pair correlation for the SSRT score

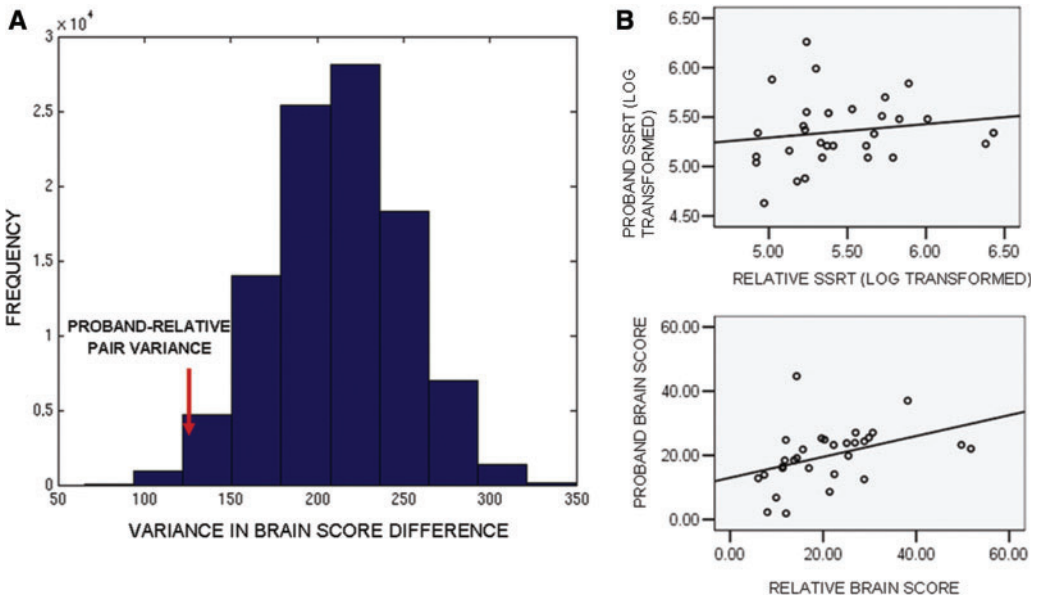

Fig. 4 Estimating familiality effects on MRI and behavioural variation in patients and their own first-degree relatives ($N = 30$ per group) (**A**) Histogram showing distribution of variance of within-pair difference in brain scores for randomly permuted pairs of patients and relatives, compared with the observed variance of within-pair difference in brain score for patients and their own relative (arrow). (**B**) Scatter plots exploring (within-pair) correlation between patients and their relatives for SSRT (top panel) and brain score (bottom panel).

($r = 0.16$, $N = 30$, $P = 0.41$) (Fig. 4B). Taken together with the results on variance of within-pair differences in MRI and cognitive phenotypes, these data suggest that compared with a behavioural measure of response inhibition, the MRI systems correlated with response inhibitory processing are more strongly determined by familial factors shared between true proband–relative pairs.

Discussion

These data provide empirical support for each of the four hypotheses motivating this study. We have confirmed that response inhibition, indexed by SSRT, is abnormal in patients with OCD and their first-degree relatives. We have identified extensive brain systems where grey matter density is (positively or negatively) correlated with variability in stop-signal task performance; and we have shown that patients with OCD and their relatives have structural abnormalities in these systems compared to healthy volunteers. Finally, we have exploited our proband–relative pair design to assess the familiality of variation in cognitive and associated MRI phenotypes and shown that variation in brain systems correlated with inhibitory function is likely determined by familial factors in common between patients and their first-degree relative. In short, we have combined structural neuroimaging and cognitive testing to identify for the first time a neurocognitive endophenotype of OCD.

Inhibition and OCD

The classical clinical symptoms of OCD are persistent, obsessional thoughts attended by an inability to inhibit compulsive behaviour repetition. It therefore seems almost self-evident that inhibitory processes might be abnormal in OCD and there is empirical evidence in support of this hypothesis. Patients with OCD are impaired across a range of tests of inhibitory function including motor inhibition tasks, e.g. go/no-go and stop-signal tasks (Bannon *et al.*, 2002; Chamberlain *et al.*, 2005, 2006; Penades *et al.*, 2006); attentional set shifting tasks, such as the object alternation task (Abbruzzese *et al.*, 1997; Aycicegi *et al.*, 2003); the intra-dimensional/extra-dimensional task (Veale *et al.*, 1996; Watkins *et al.*, 2005; Chamberlain *et al.*, 2006) which requires inhibition of a previously successful response strategy in response to changing criteria for task performance; and the Stroop task, a putative test of cognitive inhibition (van den Heuvel *et al.*, 2005*b*; Penades *et al.*, 2006). Our data, indicating that patients are impaired on a motor inhibition task, are consistent with this literature.

Brain systems associated with motor inhibition

Prior data on human brain systems underlying motor inhibition have been provided by lesion studies and neuroimaging. In a structural MRI study of patients following focal but variably located brain injuries, Aron *et al.* (2003*b*) found that grey matter volume deficit in the right inferior frontal gyrus (RIFG) was specifically predictive of prolonged SSRT; for a review of further evidence implicating the RIFG in motor inhibition see Aron *et al.* (2004). Functional neuroimaging studies of motor inhibition have generally identified a more extensive but predominantly right-sided system of regions including orbitofrontal, dorsolateral and medial frontal, temporal and parietal cortices, the cerebellum and the basal ganglia (Godefroy *et al.*, 1996; Humberstone *et al.*, 1997; Garavan *et al.*, 1999; Rubia *et al.*, 1999, 2000, 2001*a*, *b* and *c*; Horn *et al.*, 2003).

In keeping with the focus on the RIFG in previous literature, we also found evidence that reduced grey matter density in this region was associated with prolonged SSRT. However, consistent with the functional neuroimaging data suggesting involvement of a network of regions in inhibition, we found that brain areas negatively correlated with latency of inhibitory processing in our data were not restricted to the RIFG but included regions such as bilateral orbitofrontal cortex, right premotor and anterior cingulate cortex, left dorsolateral prefrontal cortex and bilateral temporal cortex. We also found a number of regions in cingulate cortex, parietal and dorsal occipital cortex, and basal ganglia where SSRT was positively correlated with grey matter density, i.e. impaired inhibitory function was predicted by increased grey matter density.

Brain systems implicated in OCD

'Affective' fronto-striatal circuits including the orbitofrontal cortex, the striatum and anterior cingulate have been invoked theoretically to account for OCD. As already discussed (Introduction, Supplementary Figs 1 and 2), there is somewhat inconsistent evidence in support of this hypothesis from structural MRI studies published to date. However, there is additional evidence for orbitofrontal dysfunction in OCD from positron emission tomography (PET) studies reporting abnormal resting or task-related orbitofrontal metabolism in OCD (Baxter *et al.*, 1987, 1988; Nordahl *et al.*, 1989; Swedo *et al.*, 1989; McGuire *et al.*, 1994; Rauch *et al.*, 1994). Functional MRI studies investigating executive function in OCD have also identified fronto-striatal abnormalities in patients (Maltby *et al.*, 2005; van den Heuvel *et al.*, 2005*a*; Remijnse *et al.*, 2006; Rauch *et al.*, 2007); and there is evidence that affective fronto-striatal circuits are abnormally activated in patients during symptom provocation (Breiter *et al.*, 1996; Adler *et al.*, 2000; Phillips *et al.*, (2000); Mataix-Cols *et al.*, 2004; Nakao *et al.*, 2005; Schienle *et al.*, 2005). Moreover, fMRI studies have often also shown changes in activation of theoretically unanticipated regions such as the dorsolateral prefrontal cortex (DLPFC) and parietal cortex. For example, van den Heuvel *et al.* (2005*a*) found decreased DLPFC activation in

OCD patients compared with controls, Maltby *et al.* (2005) found hyperactivity in the anterior and posterior cingulate and lateral prefrontal cortex during unsuccessful stopping in a go/no-go task, and Schienle *et al.* (2005) found increased activation in DLPFC and parietal areas. There is corroborative evidence for parietal cortical abnormalities in OCD from PET (Nordahl *et al.*, 1989; McGuire *et al.*, 1994; Rauch *et al.*, 1994) and SPECT (Lucey *et al.*, 1995) activation studies.

Thus our findings of extensive grey matter abnormality in orbitofrontal cortex, ventral and dorsal prefrontal cortex, cingulate cortex, parietal cortex, striatum and cerebellum include many of the regions anticipated by an orbitofronto-striatal model; but also include other regions (such as parietal cortex or cerebellum), which have been reported in the functional neuroimaging literature and by some of the prior structural MRI studies (Pujol *et al.*, 2004; Valente *et al.*, 2005; Soriano-Mas *et al.*, 2007), yet are not so readily accommodated by an exclusively orbitofronto-striatal model. As the neuroimaging evidence base grows and becomes more replicable, we predict that this will drive development of systems-level theory beyond the model of abnormality in a single cortico-striatal circuit.

Candidacy of cognitive and MRI endophenotypes of OCD

There is no universally accepted set of criteria to judge the validity of a candidate endophenotype. However, Gottesman proposed that endophenotypes are quantitative heritable traits that are abnormal in both probands and their relatives (Gottesman and Gould, 2003). How well do our data on behavioural and MRI markers of inhibitory processing satisfy these criteria?

Both behavioural and MRI markers were quantitatively abnormal on average in both patients and relatives compared to healthy volunteers. However, the demonstration of strict sense heritability is impossible in the absence of a twin design controlling for shared environmental influences on trait variation in genetically related individuals. We have therefore adopted the logistically more feasible approach of assessing familial (rather than strictly heritable) effects on trait variation in a proband–relative pair design. We have used an innovative permutation test of the within-pair variance in trait differences, and within-pair correlations, to quantify familiality of variation in discordant proband–relative pairs, finding evidence for significant familial effects on variation in the MRI systems associated with inhibitory processing, but not on the behaviourally derived SSRT measure. We conclude that the MRI markers of inhibitory processing more completely satisfy Gottesman's criteria (by virtue of their greater familiality), perhaps reflecting the fact that structural variation in brain systems is more proximal to genetic effects than variation in task performance. This result strengthens the rationale for searching for neurocognitive endophenotypes in other complex behavioural disorders such as schizophrenia and bipolar disorder.

Utility and specificity of endophenotypes of OCD

Using probands and first-degree relatives to identify MRI endophenotypes has the immediate advantage of discounting any non-familial explanations (such as exposure to psychotropic medication in the probands) for abnormal patterns of brain structure. Endophenotypes could also be used to refine diagnostic subclassification of patients (based on the extent of their expression of endophenotypic abnormality), or to highlight additional abnormalities occurring only in patients (not relatives), although these were not objectives of the current study. However, it is interesting also to consider how our results could be exploited in future to identify specific genes determining variation in brain systems important for motor inhibition. In principle, the grey matter density of the motor inhibitory system could be used as a quantitative trait in a genome-wide search for associated polymorphisms by quantitative trait locus (QTL) analysis. Although we currently lack sufficient experience of genome-wide QTL mapping based on human imaging, this has been successfully used to identify genetic markers associated with imaging measurements of cortical and subcortical grey matter volumes in inbred strains of mice (Beatty and Laughlin, 2006).

Another question concerns the diagnostic specificity of an inhibitory endophenotype for OCD. Since the present study focused on patients with predominantly classical washing/checking symptoms, these results may not generalize to other OCD subgroups. On the other hand, recent evidence has accumulated to suggest that a deficit in response inhibition may also be an endophenotype for attention-deficit/hyperactivity disorder (ADHD) (Aron and Poldrack, 2005; Crosbie and Schachar, 2001). Behavioural deficits in response inhibition have been identified in ADHD (Casey *et al.*, 1997; Vaidya *et al.*, 1998; Chamberlain and Sahakian, 2007) and previously related to abnormal activation of right inferior prefrontal cortex and left caudate during the stop-signal task (Rubia *et al.*, 1999). Clinically unaffected first-degree relatives of ADHD probands have also shown deficits on motor response inhibition in the go/no-go task (Slaats-Willemse *et al.*, 2003). Future studies of ADHD patients and their relatives would establish if impairments in response inhibition are underpinned by anatomical variation in the same brain systems that we have identified in OCD; and test that behavioural and/or imaging markers of impaired inhibitory function satisfy the Gottesman criteria as endophenotypes of ADHD. Without such data, it is speculative but intriguing to consider that the same neurocognitive endophenotype might be related to important dimensions of these two traditionally distinct clinical syndromes.

Methodological considerations

An innovative aspect of this study was the use of the PLS method, a technique previously employed mainly in the analysis of functional neuroimaging data (McIntosh and Lobaugh, 2004), to find structural brain systems optimally correlated with a behavioural variable. PLS was attractive for our purpose because there were prior theoretical reasons to expect that inhibitory deficits in OCD might be related to structural abnormalities at a systems level, rather than in a discrete brain region, and PLS is designed to optimize correlation between one or more exogenous (behavioural) variables and a set of correlated image voxels, without specifying *a priori* which voxels are likely to be components of the behaviourally correlated system. Characterization of structure–function relationships at systems level has the considerable merit of minimizing the number of significance tests required. To search for significant structure–function associations at voxel level would entail approximately 150 000 tests, with concomitantly severe thresholds for significance to mitigate the multiple comparisons problem; whereas testing for a systems level association in PLS required only one significance test, which could be thresholded conventionally at $P \leq 0.05$.

In principle, partial least squares can be used as a multivariate analysis method to explore the relationships between multiple behavioural variables and multiple imaging variables. Here we have used it to test for association between a *single* behavioural variable and grey matter density at *multiple* voxels. To distinguish this application from the more general multivariate case, where PLS is used to find associations between multiple behavioural variables and imaging measures at multiple voxels, we have referred to our application as a multivoxel analysis because the (non-parametric) test for significant association is based on behavioural correlations summed across all voxels in the brain. Thus PLS with a single behavioural variable is conceptually close to the analysis of OCD imaging data by Soriano-Mas *et al.* (2007), based on the method proposed by Worsley *et al.* (1995, 1997). The main differences are that Soriano-Mas *et al.* (2007) tested a multivoxel measure of between-group difference, whereas we have tested a multivoxel measure of continuous covariation with cognitive function across diagnostic groups. More technically, the PLS approach has the relative merit of an entirely non-parametric (resampling-based) approach to significance testing which confers greater flexibility in choice of test statistics and greater robustness against violation of the conditions required for validity of parametric tests (Worsley *et al.*, 1995, 1997).

Conclusions

To the best of our knowledge, this is the first example of a potentially powerful experimental and data analytic strategy to identify cognitive and related brain structural endophenotypes of heritable but genetically complex neuropsychiatric disorders. In a sample of OCD patients, their first-degree relatives and unrelated healthy volunteers, we have found substantial evidence that variation in motor inhibitory control is correlated with grey matter density changes in an extensive system comprising orbitofrontal, cingulate and parietal cortical areas as well as striatal and other subcortical regions. We have also tested rigorously by Gottesman's criteria the candidacy of these inhibition-related brain systems as the first neurocognitive endophenotype for obsessive-compulsive disorder.

Supplementary material

Supplementary material is available at *Brain* online.

Acknowledgements

This work was funded by the National Alliance for Research on Schizophrenia and Depression (Distinguished Investigator Award to E.B.), the Wellcome Trust (T.W.R., B.J.S.), the Harnett Fund (University of Cambridge; MB/PhD studentship to L.M.), the Medical Research Council (MB/PhD studentship to S.R.C.) and the National Institutes of Mental Health and Biomedical Imaging & Bioengineering (Human Brain Project; E.B.). The Behavioural and Clinical Neuroscience Institute is supported by a joint award from the Medical Research Council and Wellcome Trust. Mr Chamberlain and Dr Robbins and Dr Sahakian consult for Cambridge Cognition. All other authors report no competing interests. We thank Drs Randy McIntosh and Nancy Lobaugh for expert support in using their PLSGUI software. Funding to pay the Open Access publication charges for this article was provided by the Wellcome Trust.

References

Abbruzzese M, Ferri S, Scarone S. The selective breakdown of frontal functions in patients with obsessive-compulsive disorder and in patients with schizophrenia: a double dissociation experimental finding. Neuropsychologia 1997; 35: 907–12.

Adler CM, McDonough-Ryan P, Sax KW, Holland SK, Arndt S, Strakowski SM. fMRI of neuronal activation with symptom provocation in unmedicated patients with obsessive compulsive disorder. J Psychiatr Res 2000; 34: 317–24.

Alexander GE, DeLong MR, Strick PL. Parallel organization of functionally segregated circuits linking basal ganglia and cortex. Annu Rev Neurosci 1986; 9: 357–81.

Aron AR, Dowson JH, Sahakian BJ, Robbins TW. Methylphenidate improves response inhibition in adults with attention-deficit/hyperactivity disorder. Biol Psychiatry 2003a; 54: 1465–8.

Aron AR, Fletcher PC, Bullmore ET, Sahakian BJ, Robbins TW. Stop-signal inhibition disrupted by damage to right inferior frontal gyrus in humans. Nat Neurosci 2003b; 6: 115–16.

Aron AR, Poldrack RA. The cognitive neuroscience of response inhibition: relevance for genetic research in attention-deficit/hyperactivity disorder. Biol Psychiatry 2005; 57: 1285–92.

Aron AR, Robbins TW, Poldrack RA. Inhibition and the right inferior frontal cortex. Trends Cogn Sci 2004; 8: 170–7.

Ashburner J, Friston KJ. Voxel-based morphometry – the methods. Neuroimage 2000; 11: 805–21.

Atmaca M, Yildirim BH, Ozdemir BH, Aydin BA, Tezcan AE, Ozler AS. Volumetric MRI assessment of brain regions in patients with refractory obsessive-compulsive disorder. Prog Neuropsychopharmacol Biol Psychiatry 2006a; 30: 1051–7.

Atmaca M, Yildirim H, Ozdemir H, Tezcan E, Poyraz AK. Volumetric MRI study of key brain regions implicated in obsessive-compulsive disorder. Prog Neuropsychopharmacol Biol Psychiatry 2007; 31: 46–52.

Aycicegi A, Dinn WM, Harris CL, Erkmen H. Neuropsychological function in obsessive-compulsive disorder: effects of comorbid conditions on task performance. Eur Psychiatry 2003; 18: 241–8.

Aylward EH, Harris GJ, Hoehn-Saric R, Barta PE, Machlin SR, Pearlson GD. Normal caudate nucleus in obsessive-compulsive disorder assessed by quantitative neuroimaging. Arch Gen Psychiatry 1996; 53: 577–84.

Bannon S, Gonsalvez CJ, Croft RJ, Boyce PM. Response inhibition deficits in obsessive-compulsive disorder. Psychiatry Res 2002; 110: 165–74.

Baxter LR Jr, Phelps ME, Mazziotta JC, Guze BH, Schwartz JM, Selin CE. Local cerebral glucose metabolic rates in obsessive-compulsive disorder. A comparison with rates in unipolar depression and in normal controls. Arch Gen Psychiatry 1987; 44: 211–8.

Baxter LR Jr, Schwartz JM, Mazziotta JC, Phelps ME, Pahl JJ, Guze BH, Fairbanks L. Cerebral glucose metabolic rates in nondepressed patients with obsessive-compulsive disorder. Am J Psychiatry 1998; 145: 1560–3.

Bearden CE, Freimer NB. Endophenotypes for psychiatric disorders: ready for primetime? Trends Genet 2006; 22: 306–13.

Bearden CE, Reus VI, Freimer NB. Why genetic investigation of psychiatric disorders is so difficult. Curr Opin Genet Dev 2004; 14: 280–6.

Beatty J, Laughlin RE. Genomic regulation of natural variation in cortical and noncortical brain volume. BMC Neurosci 2006; 7: 16.

Breiter HC, Rauch SL, Kwong KK, Baker JR, Weisskoff RM, Kennedy DN, et al. Functional magnetic resonance imaging of symptom provocation in obsessive-compulsive disorder. Arch Gen Psychiatry 1996; 53: 595–606.

Carey G, Gottesman II. Twin and family studies of anxiety, phobic and obsessive disorders. In: Klein D, Radkin J, editors. Anxiety; new research and changing concepts. New York: Raven Press; 1981.

Casey BJ, Castellanos FX, Giedd JN, Marsh WL, Hamburger SD, Schubert AB, et al. Implication of right frontostriatal circuitry in response inhibition and attention-deficit/hyperactivity disorder. J Am Acad Child Adolesc Psychiatry 1997; 36: 374–83.

Chamberlain SR, Blackwell AD, Fineberg NA, Robbins TW, Sahakian BJ. The neuropsychology of obsessive compulsive disorder: the importance of failures in cognitive and behavioural inhibition as candidate endophenotypic markers. Neurosci Biobehav Rev 2005; 29: 399–419.

Chamberlain SR, Fineberg NA, Blackwell AD, Robbins TW, Sahakian BJ. Motor inhibition and cognitive flexibility in obsessive-compulsive disorder and trichotillomania. Am J Psychiatry 2006; 163: 1282–4.

Chamberlain SR, Fineberg NA, Menzies LA, Blackwell AD, Bullmore ET, Robbins TW, Sahakian BJ. Impaired cognitive flexibility and motor inhibition in unaffected first-degree relatives of patients with obsessive-compulsive disorder. Am J Psychiatry 2007; 164: 335–8.

Chamberlain SR, Sahakian BJ. The neuropsychiatry of impulsivity. Curr Opin Psychiatry 2007; 20: 255–61.

Choi JS, Kang DH, Kim JJ, Ha TH, Lee JM, Youn T, et al. Left anterior subregion of orbitofrontal cortex volume reduction and impaired organizational strategies in obsessive-compulsive disorder. J Psychiatr Res 2004; 38: 193–9.

Choi JS, Kim HS, Yoo SY, Ha TH, Chang JH, Kim YY, et al. Morphometric alterations of anterior superior temporal cortex in obsessive-compulsive disorder. Depress Anxiety 2006; 23: 290–6.

Crosbie J, Schachar R. Deficient inhibition as a marker for familial ADHD. Am J Psychiatry 2001; 158: 1884–90.

DuPont RL, Rice DP, Shiraki S, Rowland CR. Economic costs of obsessive-compulsive disorder. Med Interface 1995; 8: 102–9.

Foa EB, Huppert JD, Leiberg S, Langner R, Kichic R, Hajcak G, et al. The obsessive-compulsive inventory: development and validation of a short version. Psychol Assess 2002; 14: 485–96.

Garavan H, Ross TJ, Stein EA. Right hemispheric dominance of inhibitory control: an event-related functional MRI study. Proc Natl Acad Sci USA 1999; 96: 8301–6.

Gilbert AR, Moore GJ, Keshavan MS, Paulson LA, Narula V, Mac Master FP, et al. Decrease in thalamic volumes of pediatric patients with obsessive-compulsive disorder who are taking paroxetine. Arch Gen Psychiatry 2000; 57: 449–56.

Godefroy O, Lhullier C, Rousseaux M. Non-spatial attention disorders in patients with frontal or posterior brain damage. Brain 1996; 119 (Pt 1): 191–202.

Goodman WK, Price LH, Rasmussen SA, Mazure C, Fleischmann RL, Hill CL, et al. The yale-brown obsessive compulsive scale. I. Development, use, and reliability. Arch Gen Psychiatry 1989; 46: 1006–11.

Gottesman II, Gould TD. The endophenotype concept in psychiatry: etymology and strategic intentions. Am J Psychiatry 2003; 160: 636–45.

Gottesman II, Shields J. Genetic theorizing and schizophrenia. Br J Psychiatry 1973; 122: 15–30.

Graybiel AM, Rauch SL. Toward a neurobiology of obsessive-compulsive disorder. Neuron 2000; 28: 343–7.

Harrison BJ, Yucel M, Shaw M, Kyrios M, Maruff P, Brewer WJ, et al. Evaluating brain activity in obsessive-compulsive disorder: preliminary insights from a multivariate analysis. Psychiatry Res 2006; 147: 227–31.

Horn NR, Dolan M, Elliott R, Deakin JF, Woodruff PW. Response inhibition and impulsivity: an fMRI study. Neuropsychologia 2003; 41: 1959–66.

Humberstone M, Sawle GV, Clare S, Hykin J, Coxon R, Bowtell R, et al. Functional magnetic resonance imaging of single motor events reveals human presupplementary motor area. Ann Neurol 1997; 42: 632–7.

Inouye E. Similar and dissimilar manifestations of obsessive-compulsive neuroses in monozygotic twins. Am J Psychiatry 1965; 121: 1171–5.

Jenike MA, Breiter HC, Baer L, Kennedy DN, Savage CR, Olivares MJ, et al. Cerebral structural abnormalities in obsessive-compulsive disorder. A quantitative morphometric magnetic resonance imaging study. Arch Gen Psychiatry 1996; 53: 625–32.

Jenkinson M, Bannister P, Brady M, Smith S. Improved optimization for the robust and accurate linear registration and motion correction of brain images. Neuroimage 2002; 17: 825–41.

Jenkinson M, Smith S. A global optimisation method for robust affine registration of brain images. Med Image Anal 2001; 5: 143–56.

John B, Lewis KR. Chromosome variability and geographic distribution in insects. Science 1966; 152: 711–21.

Kang DH, Kim JJ, Choi JS, Kim YI, Kim CW, Youn T, et al. Volumetric investigation of the frontal-subcortical circuitry in patients with obsessive-compulsive disorder. J Neuropsychiatry Clin Neurosci 2004; 16: 342–9.

Karno M, Golding JM, Sorenson SB, Burnam MA. The epidemiology of obsessive-compulsive disorder in five US communities. Arch Gen Psychiatry 1988; 45: 1094–9.

Kim JJ, Lee MC, Kim J, Kim IY, Kim SI, Han MH, et al. Grey matter abnormalities in obsessive-compulsive disorder: statistical parametric mapping of segmented magnetic resonance images. Br J Psychiatry 2001; 179: 330–4.

Kwon JS, Shin YW, Kim CW, Kim YI, Youn T, Han MH, et al. Similarity and disparity of obsessive-compulsive disorder and schizophrenia in MR volumetric abnormalities of the hippocampus-amygdala complex. J Neurol Neurosurg Psychiatry 2003; 74: 962–4.

Lawrence AD, Sahakian BJ, Robbins TW. Cognitive functions and corticostriatal circuits: insights from Huntington's disease. Trends Cogn Sci 1998; 2: 379–88.

Leboyer M, Bellivier F, Nosten-Bertrand M, Jouvent R, Pauls D, Mallet J. Psychiatric genetics: search for phenotypes. Trends Neurosci 1998; 21: 102–5.

Logan GD, Cowan WB, Davis KA. On the ability to inhibit simple and choice reaction time responses: a model and a method. J Exp Psychol Hum Percept Perform 1984; 10: 276–91.

Lucey JV, Costa DC, Blanes T, Busatto GF, Pilowsky LS, Takei N, et al. Regional cerebral blood flow in obsessive-compulsive disordered patients at rest. Differential correlates with obsessive-compulsive and anxious-avoidant dimensions. Br J Psychiatry 1995; 167: 629–34.

Maltby N, Tolin DF, Worhunsky P, O'Keefe TM, Kiehl KA. Dysfunctional action monitoring hyperactivates frontal-striatal circuits in obsessive-compulsive disorder: an event-related fMRI study. Neuroimage 2005; 24: 495–503.

Marcelis M, Suckling J, Woodruff P, Hofman P, Bullmore E, van Os J. Searching for a structural endophenotype in psychosis using computational morphometry. Psychiatry Res 2003; 122: 153–67.

Mataix-Cols D, Wooderson S, Lawrence N, Brammer MJ, Speckens A, Phillips ML. Distinct neural correlates of washing, checking, and hoarding symptom dimensions in obsessive-compulsive disorder. Arch Gen Psychiatry 2004; 61: 564–76.

McDonald C, Bullmore ET, Sham PC, Chitnis X, Wickham H, Bramon E, et al. Association of genetic risks for schizophrenia and bipolar disorder with specific and generic brain structural endophenotypes. Arch Gen Psychiatry 2004; 61: 974–84.

McGuire PK, Bench CJ, Frith CD, Marks IM, Frackowiak RS, Dolan RJ. Functional anatomy of obsessive-compulsive phenomena. Br J Psychiatry 1994; 164: 459–68.

McIntosh AR, Bookstein FL, Haxby JV, Grady CL. Spatial pattern analysis of functional brain images using partial least squares. Neuroimage 1996; 3: 143–57.

McIntosh AR, Lobaugh NJ. Partial least squares analysis of neuroimaging data: applications and advances. Neuroimage 2004; 23 (Suppl 1): S250–63.

Montgomery SA, Asberg M. A new depression scale designed to be sensitive to change. Br J Psychiatry 1979; 134: 382–9.

Nakao T, Nakagawa A, Yoshiura T, Nakatani E, Nabeyama M, Yoshizato C, et al. Brain activation of patients with obsessive-compulsive disorder during neuropsychological and symptom provocation tasks before and after symptom improvement: a functional magnetic resonance imaging study. Biol Psychiatry 2005; 57: 901–10.

Nelson HE. National Adult Reading Test (NART) Manual. Windsor, UK, 1982.

Nestadt G, Samuels J, Riddle M, Bienvenu OJ III, Liang KY, LaBuda M, et al. A family study of obsessive-compulsive disorder. Arch Gen Psychiatry 2000; 57: 358–63.

Nordahl TE, Benkelfat C, Semple WE, Gross M, King AC, Cohen RM. Cerebral glucose metabolic rates in obsessive compulsive disorder. Neuropsychopharmacology 1989; 2: 23–8.

Pauls DL, Alsobrook JP II, Goodman W, Rasmussen S, Leckman JF. A family study of obsessive-compulsive disorder. Am J Psychiatry 1995; 152: 76–84.

Penades R, Catalan R, Rubia K, Andres S, Salamero M, Gasto C. Impaired response inhibition in obsessive compulsive disorder. Eur Psychiatry 2006.

Phillips ML, Marks IM, Senior C, Lythgoe D, O'Dwyer AM, Meehan O, et al. A differential neural response in obsessive-compulsive disorder patients with washing compared with checking symptoms to disgust. Psychol Med 2000; 30: 1037–50.

Pujol J, Soriano-Mas C, Alonso P, Cardoner N, Menchon JM, Deus J, et al. Mapping structural brain alterations in obsessive-compulsive disorder. Arch Gen Psychiatry 2004; 61: 720–30.

Rapoport JL, Wise SP. Obsessive-compulsive disorder: evidence for basal ganglia dysfunction. Psychopharmacol Bull 1988; 24: 380–4.

Rauch SL, Jenike MA, Alpert NM, Baer L, Breiter HC, Savage CR, et al. Regional cerebral blood flow measured during symptom provocation in obsessive-compulsive disorder using oxygen 15-labeled carbon dioxide and positron emission tomography. Arch Gen Psychiatry 1994; 51: 62–70.

Rauch SL, Wedig MM, Wright CI, Martis B, McMullin KG, Shin LM, et al. Functional magnetic resonance imaging study of regional brain activation during implicit sequence learning in obsessive-compulsive disorder. Biol Psychiatry 2007; 61: 330–6.

Remijnse PL, Nielen MM, van Balkom AJ, Cath DC, van Oppen P, Uylings HB, et al. Reduced orbitofrontal-striatal activity on a reversal learning task in obsessive-compulsive disorder. Arch Gen Psychiatry 2006; 63: 1225–36.

Robinson D, Wu H, Munne RA, Ashtari M, Alvir JM, Lerner G, et al. Reduced caudate nucleus volume in obsessive-compulsive disorder. Arch Gen Psychiatry 1995; 52: 393–8.

Rosenberg DR, Keshavan MS. A.E. Bennett Research Award. Toward a neurodevelopmental model of of obsessive-compulsive disorder. Biol Psychiatry 1998; 43: 623–40.

Rubia K, Overmeyer S, Taylor E, Brammer M, Williams SC, Simmons A, et al. Hypofrontality in attention deficit hyperactivity disorder during higher-order motor control: a study with functional MRI. Am J Psychiatry 1999; 156: 891–6.

Rubia K, Overmeyer S, Taylor E, Brammer M, Williams SC, Simmons A, et al. Functional frontalisation with age: mapping neurodevelopmental trajectories with fMRI. Neurosci Biobehav Rev 2000; 24: 13–9.

Rubia K, Russell T, Bullmore ET, Soni W, Brammer MJ, Simmons A, et al. An fMRI study of reduced left prefrontal activation in schizophrenia during normal inhibitory function. Schizophr Res 2001a; 52: 47–55.

Rubia K, Russell T, Overmeyer S, Brammer MJ, Bullmore ET, Sharma T, et al. Mapping motor inhibition: conjunctive brain activations across different versions of go/no-go and stop tasks. Neuroimage 2001b; 13: 250–61.

Rubia K, Taylor E, Smith AB, Oksanen H, Overmeyer S, Newman S. Neuropsychological analyses of impulsiveness in childhood hyperactivity. Br J Psychiatry 2001c; 179: 138–43.

Saxena S. Neuroimaging and the pathophysiology of obsessive compulsive disorder (OCD). In: Fu C, Senior C, Russell T, Weinberger D, Murray R, editors. Neuroimaging in Psychiatry. UK: Martin Dunitz; 2003.

Saxena S, Bota RG, Brody AL. Brain-behavior relationships in obsessive-compulsive disorder. Semin Clin Neuropsychiatry 2001; 6: 82–101.

Scarone S, Colombo C, Livian S, Abbruzzese M, Ronchi P, Locatelli M, et al. Increased right caudate nucleus size in obsessive-compulsive disorder: detection with magnetic resonance imaging. Psychiatry Res 1992; 45: 115–21.

Schienle A, Schafer A, Stark R, Walter B, Vaitl D. Neural responses of OCD patients towards disorder-relevant, generally disgust-inducing and fear-inducing pictures. Int J Psychophysiol 2005; 57: 69–77.

Sheehan DV, Lecrubier Y, Sheehan KH, Amorim P, Janavs J, Weiller E, et al. The Mini-International Neuropsychiatric Interview (M.I.N.I.): the development and validation of a structured diagnostic psychiatric interview for DSM-IV and ICD-10. J Clin Psychiatry 1998; 59 (Suppl 20): 22–33; quiz 34–57.

Slaats-Willemse D, Swaab-Barneveld H, de Sonneville L, van der Meulen E, Buitelaar J. Deficient response inhibition as a cognitive endophenotype of ADHD. J Am Acad Child Adolesc Psychiatry 2003; 42: 1242–8.

Smith SM. Fast robust automated brain extraction. Hum Brain Mapp 2002; 17: 143–55.

Soriano-Mas C, Pujol J, Alonso P, Cardoner N, Menchon JM, Harrison BJ, et al. Identifying patients with obsessive-compulsive disorder using whole-brain anatomy. Neuroimage 2007; 35: 1028–37.

Strother SC, Anderson J, Hansen LK, Kjems U, Kustra R, Sidtis J, et al. The quantitative evaluation of functional neuroimaging experiments: the NPAIRS data analysis framework. Neuroimage 2002; 15: 747–71.

Swedo SE, Schapiro MB, Grady CL, Cheslow DL, Leonard HL, Kumar A, et al. Cerebral glucose metabolism in childhood-onset obsessive-compulsive disorder. Arch Gen Psychiatry 1989; 46: 518–23.

Szeszko PR, MacMillan S, McMeniman M, Chen S, Baribault K, Lim KO, et al. Brain structural abnormalities in psychotropic drug-naive pediatric patients with obsessive-compulsive disorder. Am J Psychiatry 2004; 161: 1049–56.

Szeszko PR, Robinson D, Alvir JM, Bilder RM, Lencz T, Ashtari M. Orbital frontal and amygdala volume reductions in obsessive-compulsive disorder. Arch Gen Psychiatry 1999; 56: 913–9.

Thompson PM, Cannon TD, Narr KL, van Erp T, Poutanen VP, Huttunen M, et al. Genetic influences on brain structure. Nat Neurosci 2001; 4: 1253–8.

Vaidya CJ, Austin G, Kirkorian G, Ridlehuber HW, Desmond JE, Glover GH, et al. Selective effects of methylphenidate in attention deficit hyperactivity disorder: a functional magnetic resonance study. Proc Natl Acad Sci USA 1998; 95: 14494–9.

Valente AAJr, Miguel EC, Castro CC, Amaro EJr, Duran FL, Buchpiguel CA, et al. Regional gray matter abnormalities in obsessive-compulsive disorder: a voxel-based morphometry study. Biol Psychiatry 2005; 58: 479–87.

van den Heuvel OA, Veltman DJ, Groenewegen HJ, Cath DC, van Balkom AJ, van Hartskamp J, et al. Frontal-striatal dysfunction during planning in obsessive-compulsive disorder. Arch Gen Psychiatry 2005a; 62: 301–9.

van den Heuvel OA, Veltman DJ, Groenewegen HJ, Witter MP, Merkelbach J, Cath DC, et al. Disorder-specific neuroanatomical correlates of attentional bias in obsessive-compulsive disorder, panic disorder, and hypochondriasis. Arch Gen Psychiatry 2005b; 62: 922–33.

Veale DM, Sahakian BJ, Owen AM, Marks IM. Specific cognitive deficits in tests sensitive to frontal lobe dysfunction in obsessive-compulsive disorder. Psychol Med 1996; 26: 1261–9.

Watkins LH, Sahakian BJ, Robertson MM, Veale DM, Rogers RD, Pickard KM, et al. Executive function in Tourette's syndrome and obsessive-compulsive disorder. Psychol Med 2005; 35: 571–82.

Weissman MM, Bland RC, Canino GJ, Greenwald S, Hwu HG, Lee CK, et al. The cross national epidemiology of obsessive compulsive disorder. The Cross National Collaborative Group. J Clin Psychiatry 1994; 55 (Suppl): 5–10.

Worsley KJ, Poline JB, Friston KJ, Evans AC. Characterizing the response of PET and fMRI data using multivariate linear models. Neuroimage 1997; 6: 305–19.

Worsley KJ, Poline JB, Vandal AC, Friston KJ. Tests for distributed, nonfocal brain activations. Neuroimage 1995; 2: 183–94.

Wright IC, Sham P, Murray RM, Weinberger DR, Bullmore ET. Genetic contributions to regional variability in human brain structure: methods and preliminary results. Neuroimage 2002; 17: 256–71.

Zhang Y, Brady M, Smith S. Segmentation of brain MR images through a hidden Markov random field model and the expectation-maximization algorithm. IEEE Trans Med Imaging 2001; 20: 45–57.